Metal-Exchange Reaction on Cationic Polyiron μ_3-η^3-(C,C,O)-Ketene and μ-η^2-(C,O)-Enolate Complexes

Munetaka Akita,* Takashi Kawahara, Masako Terada, Noboru Kakinuma, and Yoshihiko Moro-oka*

Research Laboratory of Resources Utilization, Tokyo Institute of Technology, 4259 Nagatsuta, Midori-ku, Yokohama 227, Japan

Received June 15, 1988

Cationic triiron μ_3-η^3-(C,C,O)-ketene complexes, $[FP—CH_2(C{=}O{\rightarrow}FP^+)—FP]BF_4^-$, and diiron μ-η^2-(C,O)-enolate complexes, $[FP—CH_2(C{=}O{\rightarrow}FP^+)R]BF_4^-$ [FP = $(\eta^5$-$C_5R'_5)Fe(CO)_2$, $C_5R'_5$ = C_5H_5 (Cp), C_5H_4Me (Cp'), C_5Me_5 (Cp*); Fp = $CpFe(CO)_2$, Fp' = $Cp'Fe(CO)_2$, Fp* = $Cp^*Fe(CO)_2$; R = H, OMe, Ph, *p*-C_6H_4OMe], are prepared by the reactions of μ-η^2-(C,C)-ketene complexes, FP–CH_2CO–FP, and η^1-(C)-enolate complexes, FP–CH_2COR, with labile iron cations, $[FP^+(THF)]BF_4^-$, respectively. Experiments employing Fp, Fp', and Fp* as labeling agents reveal that the two iron centers bonded to the methylene terminus and the acyl oxygen atom exchange with each other via an intramolecular process. The rate of metal exchange increases as the alkyl substituents become electron donating. The equilibrium shifts to the side in which the methylene carbon is bonded to the FP group containing a less substituted cyclopentadienyl ring.

The reactivity of the ketene ligand in polymetallic systems[1] has received considerable interest as a model for a surface-bound ketene, one of the possible intermediates for the production of oxygenated compounds in the catalytic hydrogenation of carbon monoxide.[2,3] While few μ-ketene complexes are reduced by molecular hydrogen to give acetaldehyde and ethanol,[4] the cationic activation–hydridic reduction sequence[5] has been reported to be effective in the transformation of the less reactive ketene ligand into oxygenates.[6] As an example, we reported that the bridging ketene ligand in a diiron complex, Fp–CH_2CO–Fp, was converted into a vinyl ether (an enol ether of acetaldehyde) by alkylation with methyl trifluoromethanesulfonate followed by reduction with sodium borohydride.[7]

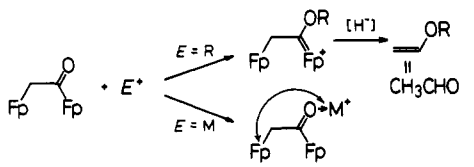

These results prompted us to activate the ketene ligand by organometallic Lewis acids instead of alkylating agents to afford cationic triiron μ_3-η^3-(C,C,O)-ketene complexes.

In the resulting triiron μ-ketene complexes we found that two of the three metal centers exchanged with each other. Since the starting and the resulting μ-ketene complexes are formally regarded as transition-metal *C*- and *O*-enolates,[8] the observed phenomenon may provide a clue to the reaction mechanism in the transmetalation of enolato ligands.

We describe herein full details of the preparation and reactivities of cationic triiron μ-ketene complexes and related complexes.[9]

Results and Discussion

Preparation of the Cationic Triiron μ_3-η^3-(C,C,O)-Ketene Complex 3a. The ligand-exchange reaction of a coordinatively labile iron cation, $[Fp^+(THF)]BF_4^-$ (**2a**), with a diiron μ-η^2-(C,C)-ketene complex, **1a**, in dichloromethane gave deep purple-red microcrystals of **3a** in 65% yield after recrystallization from diethyl ether–dichloromethane (eq 1).[10] The reaction proceeded under milder

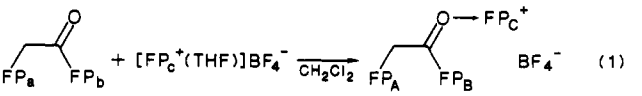

(1)

1a–d **2a–c** **3a–g**

FP_a	FP_b		FP_c		FP_A	FP_B	FP_C		
Fp	Fp	(**1a**)	Fp	(**2a**)	Fp	Fp	Fp	(**3a**), 65%	
Fp	Fp'	(**1b**)	Fp'	(**2b**)	Fp	Fp'	Fp	(**3b**), 56%	
Fp'	Fp	(**1c**)	Fp	(**2c**)	Fp'	Fp	Fp	(**3c**), 48%	from **1a**
Fp*	Fp	(**1d**)			Fp	Fp	Fp'	(**3d**), 58%	from **1c**
					Fp*	Fp	Fp	(**3e**), 74%	from **1a**
					Fp	Fp	Fp*	(**3f**), 58%	from **1d**
					Fp*	Fp	Fp*	(**3g**), 62%	

conditions compared with that of mononuclear complexes (cf. Fp–$COCH_3$, refluxing in CH_2Cl_2 for 1–6 h) because the nucleophilicity of the acyl oxygen atom in **1a** was enhanced owing to the so-called β-effect as revealed by an IR study (the red shift of ν(C=O))[7] and X-ray crystallography.[11]

Spectroscopic features of the product **3a** described below (Table I) are consistent with the structure **3** (an μ_3-η^3-(C,C,O)-ketene complex)[12] incorporating the oxycarbene

(1) Geoffroy, G. L.; Bassener, S. L. *Adv. Organomet. Chem.* **1988**, *28*, 1.

(2) (a) Blyholder, G.; Emmet, P. H. *J. Phys. Chem.* **1960**, *64*, 470. (b) Ichikawa, M.; Sekizawa, K.; Shikakura, K.; Kawai, M. *J. Mol. Catal.* **1981**, *11*, 167. (c) Takeuchi, A.; Katzer, J. R. *J. Phys. Chem.* **1982**, *86*, 2438. (d) McBreen, P. H.; Erley, W.; Ibach, H. *Surf. Sci.* **1984**, *148*, 292.

(3) (a) Masters, C. *Adv. Organomet. Chem.* **1979**, *19*, 63. (b) Muetterties, E. L.; Rhodin, T. N.; Band, E.; Brucker, C. F.; Pretzer, W. R. *Chem. Rev.* **1979**, *79*, 91. (c) Rofer-DePoorter, C. K. *Ibid.* **1981**, *81*, 447. (d) Herrmann, W. A. *Angew. Chem., Int. Ed. Engl.* **1982**, *21*, 117.

(4) Morrison, E. D.; Steinmetz, G. R.; Geoffroy, G. L.; Fultz, W. C.; Rheingold, A. L. *J. Am. Chem. Soc.* **1984**, *106*, 4783.

(5) Brookhart, M.; Tucker, J. R.; Husk, G. R. *J. Am. Chem. Soc.* **1983**, *105*, 258.

(6) (a) Bassner, S. L.; Morrison, E. D.; Geoffroy, G. L.; Rheingold, A. L. *J. Am. Chem. Soc.* **1986**, *108*, 5358. (b) *Organometallics* **1987**, *6*, 2207.

(7) (a) Akita, M.; Kondoh, A.; Moro-oka, Y. *J. Chem. Soc., Chem. Commun.* **1986**, 1296. (b) Akita, M.; Kondoh, A.; Kawahara, T.; Moro-oka, Y. *J. Organomet. Chem.* **1987**, *323*, C43. (c) Akita, M.; Kondoh, A.; Kawahara, T.; Takagi, T.; Moro-oka, Y. *Organometallics* **1988**, *7*, 366.

(8) (a) Burkhardt, E. R.; Doney, J. J.; Bergman, R. G.; Heathcock, C. H. *J. Am. Chem. Soc.* **1987**, *109*, 2022. (b) Burkhardt, E. R.; Doney, J. J.; Stack, J. G.; Bergman, R. G. *J. Mol. Catal.* **1987**, *41*, 41.

(9) Preliminary reports of some of aspects of this work have appeared. (a) Akita, M.; Kawahara, T.; Moro-oka, Y. *J. Chem. Soc., Chem. Commun.* **1987**, 1356. (b) Akita, M.; Terada, M.; Moro-oka, Y. *J. Organomet. Chem.* **1988**, *345*, C9.

(10) LaCroce, S. J.; Cutler, A. R. *J. Am. Chem. Soc.* **1982**, *104*, 2312.

(11) Akita, M.; Kondoh, A.; Moro-oka, Y. *J. Chem. Soc., Dalton Trans.*, in press.

(12) Holmgren, J. S.; Shapley, J. R.; Wilson, S. R.; Pennington, W. T. *J. Am. Chem. Soc.* **1986**, *108*, 508.

0276-7333/89/2308-0687$01.50/0

Scheme I. Formation of Cationic Triiron μ-Ketene Complexes 3 by Using Fp′ and Fp* Groups as Labeling Agents

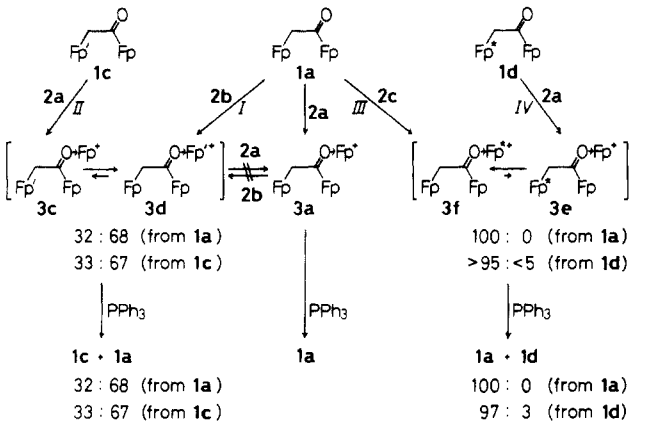

resonance form **4** and the π-complex resonance form **5**, with the largest contribution being ascribed to **4** (eq 2).

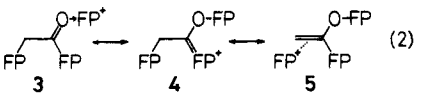

(2)

(i) ^1H and ^{13}C NMR spectra reveal the presence of three nonequivalent Fp groups and a ketene bridge. (ii) The absence of the ν(C=O) absorption in the range of 1800–1500 cm^{-1} indicates coordination of the acyl oxygen atom to a Lewis acid. (iii) The acyl carbon atom (δ 297.46) is observed in the region of cationic oxycarbene carbons of closely related mono- and dinuclear complexes such as $Fp^+{=}C(OMe)CH_3CF_3SO_3^-$ (δ 334.30) and $Fp{-}CH_2C(OMe){=}Fp^+CF_3SO_3^-$ (δ 299.07).[7c] In addition, the molecular ion peak of the cationic part of **3a** (m/z 537) can be observed by FDMS.

While **3a** (an activated form of **1a**) readily reacted with nucleophiles such as PPh_3 and $NaBH_4$ to produce $[Fp^+(PPh_3)]BF_4^-$ and Fp_2, respectively, in addition to **1a**, no trace of the products arising from the net reduction of the acyl C=O bond in **1a** could be detected even by ^1H NMR experiments (eq 3). These products can be accounted for

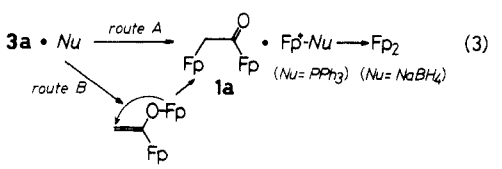

(3)

by direct removal of Fp_C by nucleophiles (route A) and removal of Fp_A followed by an O-to-C metal migration (route B).

Metal-Exchange Reaction Confirmed by Labeling Experiments Using Fp′ and Fp* Groups. To determine the regiochemistry of the nucleophilic attack and to assign the NMR signals, we attempted labeling experiments using Fp′ group (Scheme I). Of the three Cp absorptions (^1H NMR) of **3a** the signal appearing at the highest field was readily assigned to Cp_B by comparison with **3b** (obtained by the reaction between **1b** and **2a**). Attempts to distinguish the FP_A and FP_C parts by the reaction of **1a** with **2b** (reaction I) and the reaction of **1c** with **2a** (reaction II) resulted in the formation of mixtures of products. Figure 1 shows the ^1H and ^{13}C NMR spectra of the products of reaction I, and an apparently identical spectrum is obtained for reaction II. The complicated absorptions can be divided into two sets, A and B (A/B = 68/32 for reaction I and 67/33 for reaction II), which can be attributed to an isomeric pair of triiron μ-ketene complexes **3c** and

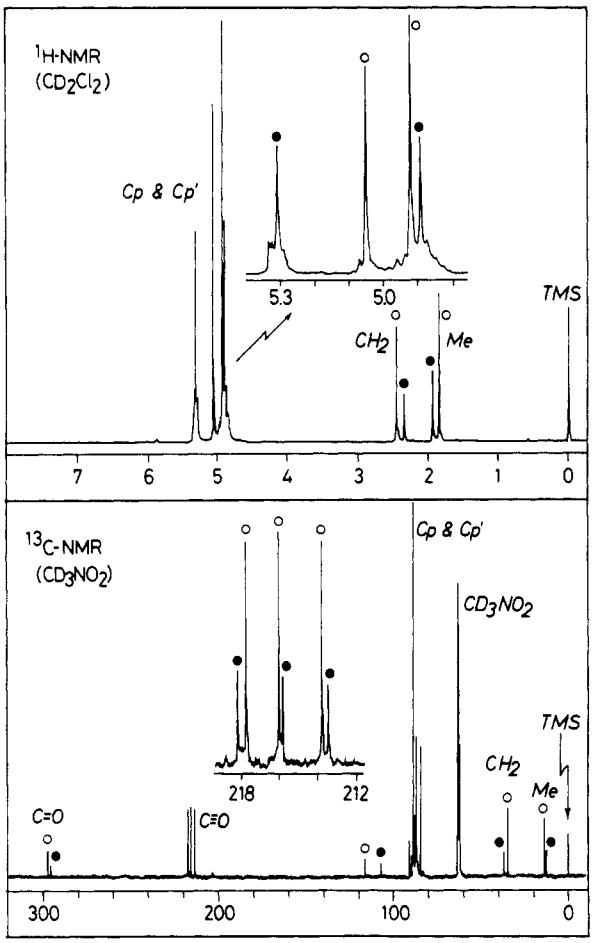

Figure 1. ^1H and ^{13}C NMR spectra of an equilibrated mixture of **3c** and **3d**: A set, ○ (**3d**); B set, ● (**3c**).

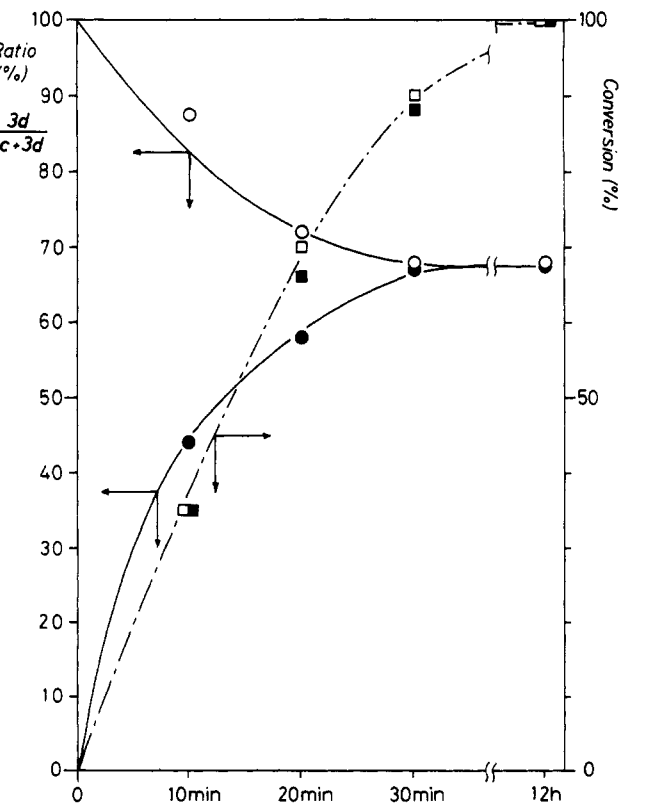

Figure 2. The changes in conversion (squares) and isomer ratio (circles) during the reaction I and II as a function of time: open marks, reaction I (**1a** + **2b**); closed marks, reaction II (**1c** + **2a**). Conditions: [1] = [2] = 0.2 M, at 27 °C.

Table I. ^{1}H NMR Spectral Data for Ketene and Enolate Complexes[a]

complex	Cp_C	Cp_A	Cp_B	other CP's	CH_2	R
3a[b]	5.30	5.07	4.89		2.44	
3b[b]	5.30	5.07		1.93, 4.14–4.80 (m)	2.44	
3c[b]	5.31		4.89	1.94[c]	2.34	
3d[b]		5.05	4.92	1.85[c]	2.45	
3e[b]	5.30		4.86	1.73	2.20	
3f[b]		5.02	4.91	1.76	2.42	
3g[b,d]			4.89	1.73	1.88	
	5.30–5.31	5.02–5.07	4.86–4.92			
7a[e]		5.04		1.73	1.66	3.77
9a[e]	5.22			1.76	1.13	3.75
7b[e]		5.10		1.74	1.99 (d, 6.6)	8.42 (t, 6.6)
9b[e]	5.30			1.79	1.64 (t, 6.3)	8.10 (t, 6.3)
7c[e]		4.96		1.75	2.46	7.42–4.58 (m)
9c[e]	5.33					
7d[e]		4.99		1.75	2.40	3.85, 6.90 (d, 8.8), 7.57 (d, 8.8)
9d[e]	5.27					
1d[f]		4.47		1.38	2.33	
8a[f]				1.33	1.39	3.60
8b[f]				1.33	1.48 (d, 5.3)	9.59 (t, 5.3)
8c[f]				1.36	2.16	7.19–7.28 (m, 3 H), 8.06–8.16 (m, 2 H)
8d[f]		4.13			2.34	3.24, 6.79 (d, 9.0), 7.82 (d, 9.0)
6d[f]				1.39	2.17	3.27, 6.81 (d, 9.0), 8.13 (d, 9.0)

[a] Observed at 100 MHz at 27 °C. Chemical shifts in δ. Values in parentheses are multiplicity and coupling constants. Unless otherwise stated, signals are singlet. [b] In CD_2Cl_2. [c] Signals due to Cp′ ring protons appear as multiplet around δ 4.8–5.1. [d] CH_2Cl_2, δ 5.37. [e] In $CDCl_3$. [f] In C_6D_6.

3d because of the presence of the Cp_B signals. In Figure 2 the conversion of the starting complexes and the isomer ratio (estimated from the integral ratios of the CH_2 absorptions of the ketene bridge) are plotted against the reaction time. The starting complexes are almost consumed within 30 min. Extrapolation of the curves of the isomer ratio A/B to $t = 0$ indicates that at the initial stage reactions I and II afford adducts A and B, respectively. On the assumption that the initial products are simple coordination complexes between **1** and **2**, A and B are assigned to **3d** and **3c**, respectively. These results demonstrate that FP_A and FP_C on **3** exchange with each other after initial coordination and that the Cp signals of **3a** observed in the middle field and the lowest field are attributed to Cp_A and Cp_C, respectively. In addition, since both reactions I and II finally produce a mixture of **3c** and **3d** in the same ratio, the present metal-exchange reaction attains an equilibrium. When an equilibrated mixture of **3c** and **3d** (32:68) was treated with a small excess amount of PPh_3, diiron μ-ketene complexes **1c** and **1a** were regenerated in the same ratio (32:68). These labeling experiments also reveal that nucleophiles attack FP_C to release FP_A–CH_2CO–FP_B (route A in eq 3).

We conclude that the metal-exchange reaction proceeds via an intramolecular reaction pathway by examining the incorporation of externally added cations. The isolated triiron μ-ketene complex is stirred with an iron cation containing a different Cp group for 12 h (eq 4 and 5).

$$\mathbf{3a} \xrightarrow[(2)\ PPh_3]{(1)\ \mathbf{2b}/CH_2Cl_2,\ 12\ h} \underset{96:4}{\mathbf{1a} + \mathbf{1c}} \qquad (4)$$

$$\underset{66:34}{\mathbf{3d} + \mathbf{3c}} \xrightarrow[(2)\ PPh_3]{(1)\ \mathbf{2a}/CH_2Cl_2,\ 12\ h} \underset{68:32}{\mathbf{1a} + \mathbf{1c}} \qquad (5)$$

Since it is difficult to analyze the complicated ^{1}H NMR spectrum of the reaction mixture, the extent of incorporation is determined by the change in the ratio **1c**/**1a** after removal of FP_c by the treatment with PPh_3. The reaction of **3a** with **2b** resulted in the formation of a 96:4 mixture of **1a** and **1c**, and the reaction of an equilibrated mixture of **3d** and **3c** (66:34) with **2a** gave **1a** and **1c** in a 68:32 ratio. Thus, less than 4% of the added cations are incorporated. This conclusion is supported by the fact that reactions I and II do not afford all four possible products (**3a**, **3c**, **3d**, and [Fp′—CH_2(C=O→Fp′$^+$)—Fp]BF_4^-), but only two products (**3c** and **3d**).

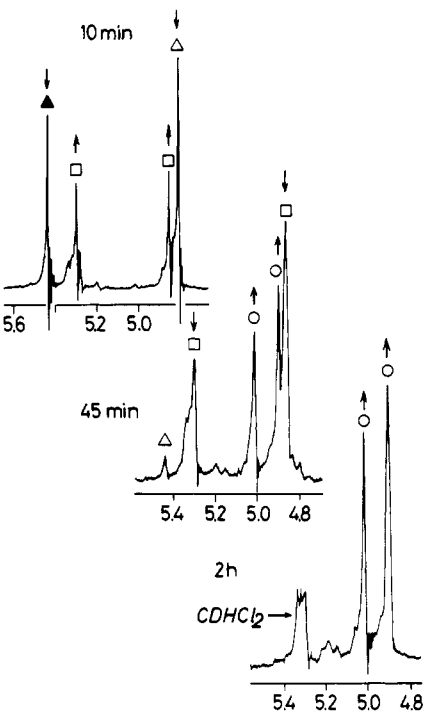

Figure 3. ^{1}H NMR (60 MHz) spectral changes during the reaction IV (**1d** + **2a**): **1d** (△), **2a** (▲), **3e** (□), **3f** (○). Conditions: [**1d**] = [**2a**] = 0.2 M, at 27 °C.

Labeling experiments using Fp* groups also confirm the metal-exchange reaction on the ketene ligand (Scheme I). Both the reaction of **1a** with **2c** (reaction III) and the reaction of **1d** with **2a** (reaction IV) afford **3f** as a sole product. The spectral changes in the Cp region during reaction IV are reproduced in Figure 3. The structure of intermediate **3e** whose signals are marked with squares is readily assigned on the basis of the chemical shifts of the Cp signals (Table I). The remarkable difference between Fp′ and Fp* systems is that the equilibrium almost completely shifts to one side. The addition of PPh_3 to the

Table II. ^{13}C NMR Spectral Data for Ketene and Enolate Complexes[a]

complex	Cp	Cp*, Cp′	CH_2	C=O	C≡O
3a[b]	88.18 (d, 183.1), 88.76 (d, 181.6)[c]		33.33 (t, 139.7)	297.46	213.10, 215.44, 217.50
3b[b]	88.37	13.40, 87.11, 91.31, 107.53	33.61	299.24	213.46, 216.20, 217.79
3c[b]	88.44, 89.03	13.53,[d] 116.61	36.91	296.63	213.47, 215.82, 218.17
3d[b]	88.34, 88.74	12.85,[d] 107.06	34.50	297.90	213.74, 215.98, 217.69
3f[e]	87.25 (d, 181.2), 87.44 (d, 181.2)	9.73 (q, 128.7), 99.60	33.90 (t, 138.3)	295.51	213.97, 214.65, 216.24
3g[e,f]	87.16 (d, 181.9)	9.38 (q, 128.1), 9.76 (q, 129.1), 97.89, 99.91	48.06 (t, 137.2)	291.93	214.23, 215.28, 217.99
7a[g]	85.96 (d, 182.0)	9.27 (q, 129.1), 98.23	−7.10 (t, 143.1)	197.86	212.14, 214.27
9a[g]	85.72 (d, 183.4)	9.40 (q, 129.1), 96.80	2.98 (t, 141.6)	199.15	210.25, 215.93
7b[g]	85.19 (d, 182.8)	9.31 (q, 129.3), 98.64	15.07 (dt, 19.1, 147.8)	208.14 (d, 173.2)	211.84, 213.36
9b[g]	86.06 (d, 184.4)	9.45 (q, 128.7), 97.05	25.71 (dt, 18.5, 147.0)	206.57 (d, 171.7)	210.01, 215.23
7c[g,h]	86.14 (d, 182.1)	9.24 (q, 129.1), 99.37	8.07 (t, 142.3)	220.41	212.56, 213.51
7d[g,i]	86.38 (d, 181.5)	9.52 (q, 129.0), 99.42	7.70 (t, 142.5)	220.00	212.92, 213.91
1d[j]	87.27 (d, 178.9)	9.02 (q, 127.7), 95.09	42.61 (t, 134.5)	250.64	217.35, 218.86
8a[j]		8.93 (q, 128.0), 95.22	4.07 (t, 137.7)	183.05	217.82
8b[j]		8.91 (q, 127.7), 95.60	19.19 (dt, 28.4, 137.2)	199.14 (td, 4.0, 161.4)	217.85
8c[j,k]		9.05 (q, 127.6), 95.48	12.40 (t, 135.8)	204.92	217.68
8d[j,l]		9.05 (q, 127.7), 95.48	12.29 (t, 135.8)	204.11	217.87
6d[j,m]	86.22 (d, 180.8)		2.23 (t, 137.9)	204.98	216.33

[a] Observed at 68 MHz at 27 °C. Chemical shifts in δ. [b] In CD_3NO_2. [c] Two Cp's are overlapping. [d] Other signals cannot be resolved due to overlapping. [e] In CD_2Cl_2. [f] CH_2Cl_2, δ 53.81 (t, 177.6). [g] In $CDCl_3$. [h] Ph: δ 126.02 (td, 6.4, 161.6), 128.57 (td, 7.7, 162.7), 132.63 (td, 7.7, 161.5), 138.91 (t, 7.7). [i] p-C_6H_4OMe: δ 55.57 (q, 144.7), 113.95 (dd, 4.7, 162.7), 128.85 (dd, 6.7, 160.0), 131.58 (s), 163.54 (s). [j] In C_6D_6. [k] Ph: δ 128.04 (td, 6.6, 160.0), 128.27 (dd, 7.3, 159.9), 131.14 (td, 7.3, 159.9), 140.02 (s). [l] p-C_6H_4OMe: δ 54.74 (q, 143.8), 113.51 (dd, 4.7, 158.7), 130.06 (dd, 7.4, 160.0), 132.69 (s), 162.45 (s). [m] p-C_6H_4OMe: δ 54.78 (q, 143.6), 113.61 (d, 160.3), 130.14 (d, 161.4), 132.15 (s), 162.78 (s).

equilibrated mixture liberated **1a** and **1d** in a 95:5 (or greater) ratio.

The results of labeling experiments using Fp′ and Fp* groups are summarized in Scheme I. Two conclusions can be drawn from the experiments. First, the equilibrium shifts to the side in which iron groups containing the more substituted Cp ring (less Lewis acidic center) occupy the FP_C position. Second, as the difference in Lewis acidity of the exchanging two iron centers increases, the equilibrium shifts to one side. Replacement of Fp′ with Fp* results in a change in the isomer ratio from 2:1 to greater than 20:1.

Preparation and Metal-Exchange Reaction of μ-η²-(C,O)-Enolate Complexes. Taking into account the three limiting resonance structures **3–5** as possible factors determining the equilibrium of the present metal-exchange reaction, we examined whether the FP_B group is essential to the metal-exchange reaction. Several isomeric pairs of μ-η²-(C,O)-enolate complexes **7** and **9**, in which FP_B of the triiron μ-ketene complex was replaced with organic substituents, were generated as shown in eq 6, and the exchange reaction was tested similarly.

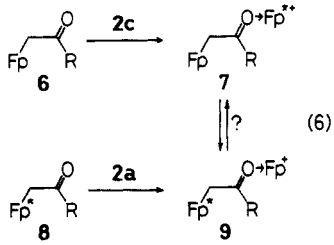

(6)

R= OMe(**a**), H(**b**), Ph(**c**), p-C_6H_4-OMe(**d**)

Complexes **6** and **8** were prepared by the esterification of the corresponding carboxylic acids (**a**)[7c] and the alkylation of the corresponding ferrates with acetal or ketals of the α-halo aldehyde or α-halo ketones followed by acidic hydrolysis (**b–d**).[13] The electron-donating ability of the substituents can be evaluated on the basis of ν(C=O) and

(13) Cutler, A.; Raghu, S.; Rosenblum, M. *J. Organomet. Chem.* **1974**, *77*, 381.

Table III. Correlation between ν(C=O) Absorptions of Ketene and Enolate Complexes and the Rate of the Metal-Exchange Reaction

	ν(C=O),[a] cm^{-1}				
R	**6**	**7**	exchange reaction ($t_{1/2}$)[b]	**9**	**8**
MeO (**a**)	1675	1562	no	1560	1677
H (**b**)	1650	1558	no	1546	1641
Ph (**c**)	1621	1521	yes (5 h)		1618
p-C_6H_4OMe (**d**)	1616	1514	yes (3 h)		1619
Fp	1612 (**1a**)	1443 (**3f**)[c]	yes (0.5 h)		1607 (**1d**)

[a] Observed in CH_2Cl_2. [b] Approximate half-lives of **9** (**3e**). [c] The absorption of medium intensity is tentatively assigned.

δ(C=O) values (Tables II and III) as follows: MeO (**a**) < H (**b**) < Ph (**c**) < p-$MeOC_6H_4$ (**d**) < Fp (**1**). **6** and **8** subsequently were converted to isomeric pairs of μ-η²-(C,O)-enolate complexes **7** and **9** by treatment with appropriate iron cations and the products isolated as deep red crystals or a deep red oil. The red shift of ν(C=O) by ca. 100 cm^{-1} demonstrates the coordination occurring on the acyl oxygen atom. The cationic character of the products is indicated by the shift of ν(C≡O) to slightly higher energies.

For R = MeO (**a**) and H (**b**) two regioisomers, **7** and **9**, were separately isolated in pure form by the reaction of **6** and **2c** and the reaction of **8** and **2a**, respectively. However, when R was an aromatic group (**c** and **d**), only one of two isomers of **7** was ultimately obtained irrespective of the preparative routes (**6** + **2c** or **8** + **2a**). Thus, in the cases of the **c** and **d** series metal-exchange reaction takes place, and **9c** and **9d** can be observed by monitoring the reactions of **8c** and **8d** with **2a** in CD_2Cl_2 by ^1H NMR. The structures of **9c** and **9d** can be unequivocally assigned on the grounds of the chemical shift of the Cp signals (the Cp_B region). The consumption of the reactants and the isomer ratios during the reaction are shown in Figure 4 accompanied by the results for the μ-ketene complex. While no significant difference in the rate of adduct formation is observed, the rate of the metal-exchange reaction estimated by approximate half-lives varies in the order MeO, H ≪ Ph (5 h) < p-$MeOC_6H_4$ (3 h) ≪ Fp (0.5 h). This

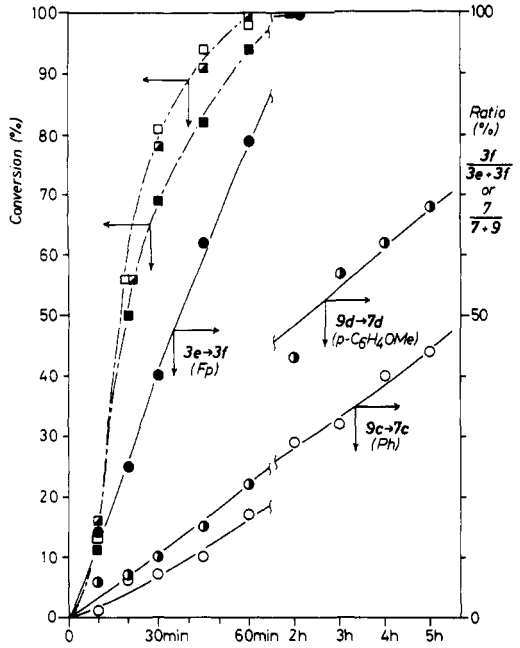

Figure 4. The changes in conversion (squares) and isomer ratio (circles) during reactions of **1d** and **8c,d** with **2a** as a function of time: closed marks, **1d** + **2a**; half closed marks, **8d** + **2a**; open marks, **8c** + **2a**. Conditions: [**1d**] = [**8**] = [**2a**] = 0.2 M, at 27 °C.

order shows good agreement with that of the electron-donating ability of the substituents estimated by the shift in ν(C=O) (Table III). We concluded that the electron-donating substituent on the acyl carbon of the μ-η^2-(C,O)-enolate complex brings about the metal-exchange reaction.

Preparation of Heterometallic Complexes. A heterometallic μ_3-η^3-(C,C,O)-ketene complex, **11**, was prepared by acidolysis of Cp_2ZrMe_2 with **10** (a conjugated acid of **1a**). The reaction was accompanied by rapid gas evolution (methane) (eq 7). The observation of the acyl carbon

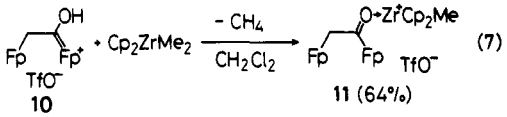

signal at a lower field by ca. δ 15 compared to that in **3** indicates the enhanced contribution of the oxycarbene structure corresponding to **4** due to the well-known oxygenophilicity of Zr. When acetone was added to a CH_2Cl_2 solution of **11**, C–C bond formation at the methylene terminus was not observed. Instead acetone inserted into the Zr–Me bond giving *t*-BuOH after hydrolysis.

Although preparation of heterometallic μ-η^2-(C,O)-enolate complexes containing cationic $CpMo(CO)_3$,[14] $Rh(CO)(PPh_3)_2$,[15] and $Mn(CO)_5$[16] fragments was also attempted, no pure products could be isolated. The molybdenum system showed an indication of the metal-exchange reaction (eq 8). The reaction of $CpMo(CO)_3CH_2COPh$ (**12**) with **2a** gave cationic products. Treatment of the product with PPh_3 released **12** and **6c**, the ratio of which changed from 6.4:1 (1 h) to 1:2.5 (72 h). If it is assumed that **11** and **6c** originate from heterobimetallic μ-enolate complexes $CpMo(CO)_3$—CH_2(C=O→Fp^+)—Ph and Fp—CH_2(C=O→$Mo^+Cp(CO)_3$)—Ph, the Mo group moves from the methylene carbon to the acyl oxygen atom.

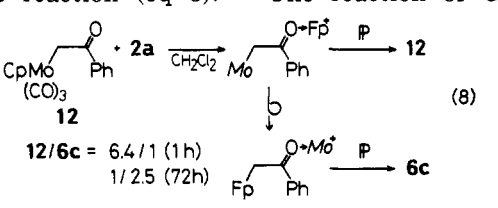

Scheme II. A Plausible Reaction Mechanism for the Metal-Exchange Reaction

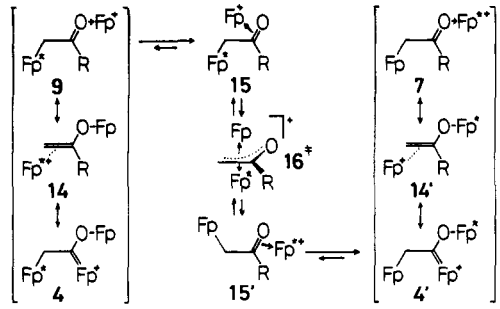

Mechanism of Metal-Exchange Reaction. The cationic diiron μ-η^2-(C,O)-enolate complex exhibits chemical behavior similar to that of the cationic diiron μ-allyl complex **13** (eq 9) and can be regarded as its oxa analogue. **13**,

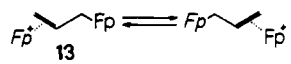

initially prepared by King,[17] has been reported to be fluxional. Only one Cp resonance (^{1}H NMR) is observed even at −90 °C, while the cationic and the neutral part are readily distinguishable in its IR spectrum.[18] Similar results have been observed for substituted allyl complexes as reported by Rosenblum.[19] In the solid state the two metal centers are bound almost identically to the bridging allyl ligand.[20] These observed phenomena are consistent with the fast equilibrium shown in eq 9.

The results described above are interpreted by a reaction mechanism depicted in Scheme II. The σ-coordinated acyl group **9** is initially converted into the π-coordinated one **15**. The metal-exchange reaction may take place via a transition state, **16**, in which the bridging enolate (oxaallyl) ligand is put between the two metal centers. Presumably because of the additional acctivation energy required for converting **9** to **15**, **9** is not fluxional even at room temperature.

Electron-releasing substituents stabilize the transition state **16** by neutralizing the positive charge on the cationic metal center and consequently enhance the rate of isomerization. The organometallic substituent Fp provides electron density by means of the oxycarbene resonance form **4** as suggested by the changes in ν(C=O) and δ(C=O) during the adduct formation [ν(C=O) (**1**, **6**, **8**) − ν(C=O) (**3**, **7**, **9**) = 92–117 cm^{-1} for **6** and **8** and >160 cm^{-1} for **1**; ν(C=O) (**3**, **7**, **9**) − δ(C=O) (**1**, **6**, **8**) = 6.8–17.5 ppm for **6** and **8** and 42 ppm for **1**]. It is difficult for most organic substituents to cause π-electron delocalization to the extent

(14) Beck, W.; Schloter, K. *Z. Naturforsch.* **1978**, *33B*, 1214.
(15) Peone, J., Jr.; Flynn, B. R.; Vaska, L. *Inorg. Synth.* **1974**, *15*, 71.
(16) Lesch, D. A.; Richardson, J. W.; Jacobson, R. A.; Angelici, R. J. *J. Am. Chem. Soc.* **1984**, *106*, 2901.
(17) King, R. B.; Bisnette, M. B. *J. Organomet. Chem.* **1967**, *7*, 311.
(18) Kerber, R. B.; Giering, W. P.; Bauch, T.; Waterman, P.; Chou, E.-H. *J. Organomet. Chem.* **1976**, *120*, C31.
(19) Priester, W.; Roseblum, M.; Samuels, S. B. *Synth. React. Inorg. Met.-Org. Chem.* **1981**, *11*, 525.
(20) Laing, M.; Moss, J. R.; Johnson, J. *J. Chem. Soc., Chem. Commun.* **1977**, 656.
(21) The measurement of activation parameters of **3a** by ^{1}H NMR techniques (saturation transfer and coalescence at higher temperature) was prevented by contamination with a very small amount of paramagnetic impurities, low solubility to high-boiling solvents such as $CDCl_3$, and nucleophilic displacement with donating solvents such as CD_3NO_2 at higher temperature.

Scheme III. Possible Reaction Pathways for Transmetalation of a η^1-(C)-Enolato Ligand

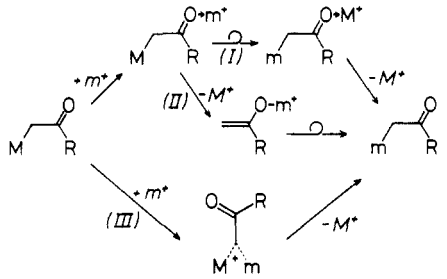

brought about by Fp ($p\pi$–$d\pi$ back-donation).

Of the two pairs of isomers (**9**, **7**, and **14**, **14′**), it is expected that **9** and **14′** should be more stable than **7** and **14**, respectively, because the thermodynamic stability of isomers is governed by the strength of the ligand-to-metal donation. (In **9** and **14′**, the more Lewis acidic metal center Fp is coordinated by electron-donating ligands with the Fp* group.) In fact, the labeling experiments clarified that the equilibrium is shifted to the right side. Therefore, the π-complex resonance form **14′** plays a dominant role in determining the equilibrium. The steric effect may be another possible driving force, but we have not succeeded in preparing iron complexes with an electron-withdrawing Cp group such as η^5-C_5H_4I and η^5-C_5H_4COR.[22]

Since **7** (**9**) and **14** can be formally regarded as coordination complexes of a metal *C*-enolate and a π-complex of a metal *O*-enolate, respectively, and the tendency observed for the metal-exchange reaction coincides with that of the transmetalation of alkyl ligands [M–R + m–X → m–R + M–X: alkyl groups migrate from a more electropositive metal (M) to a less electropositive metal (m)],[23] the μ-enolate complexes **7** and **9** may be regarded as one of many possible intermediates in the transmetalation and the interconversion of *C*- and *O*-enolates. The isomerization between metal *C*- and *O*-enolates has been studied because in some cases the stereoselectivity in the aldol condensation is dominated by the isomer ratio as typically exemplified for stannyl enolates.[24] However, there have been reported few reaction mechanisms accounting for the transmetalation of an enolate ligand (other than a 1,3-migration) presumably because labeling experiments of metal ions such as Li^+ and Na^+ are difficult. Hence we now postulate path I as one of many possible reaction pathways for the transmetalation of η^1-(C)-enolato ligands (Scheme III).

In addition, an oxycarbene structure should be considered (eq 10), when a ketene species is generated on a

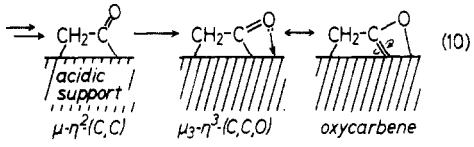

(10)

catalyst surface consisting of transition-metal components and acidic support such as a Rh/ZrO_2 system, which is known to catalyze the selective conversion of syngas to C_2 oxygenates.[26] The exchange reaction also provides a plausible explanation for mobility of a surface ketene species; i.e., a η^3-ketene species may pivot around the M–C(acyl) bond.

Experimental Section

General Data. All manipulations were performed under argon atmosphere by using standard Schlenk tube techniques. Analytical techniques have been described in our previous paper.[7c] IR spectra were recorded as CH_2Cl_2 solutions unless otherwise stated. Solvents were dried over appropriate drying agents, distilled, and stored under argon: THF (tetrahydrofuran), ether, hexane, Na/K benzophenone; CH_2Cl_2, P_2O_5. **1a–c**,[7c] **2a**,[26] **2c**[27] **8a**,[7c] Fp_2,[28] Fp^-,[28] Fp^*_2,[27] Fp^{*-},[29] Cp_2ZrMe_2[30] were prepared according to the published methods.

Preparation of 1d. **1d** was prepared from Fp^*CH_2COOH[31] (2.50 g, 8.17 mmol) and Fp_2 (1.74 g, 4.9 mmol) according to our previous report[7c] in 50% yield (1.90 g, 4.08 mmol). **1d**: yellow crystals. Anal. Calcd for $C_{21}H_{22}O_5Fe_2$: C, 54.11; H, 4.76. Found: C, 54.52; H, 4.80. IR: 2001, 1987, 1943 cm^{-1}.

Preparation of 2b. **2b** was prepared from Fp′I (2.84 g, 8.93 mmol) and $AgBF_4$ (1.89 g, 9.67 mmol) in THF (45 mL).[26] **2b** (1.71 g, 1.61 mmol, 55% yield): red powder; mp 82–84 °C. Anal. Calcd for $C_{12}H_{15}BF_4O_3Fe_2$: C, 41.19; H, 4.32. Found: C, 40.80; H, 4.10. ^1H NMR (CD_2Cl_2): δ 1.82 (s, 3 H, Me), 1.84, 3.50 (m, 4 H × 2, THF), 5.12–5.42 (m, 4 H, C_5H_4Me). IR (KBr): 2042, 1990 cm^{-1}.

Preparation of Triiron μ-Ketene Complexes 3. **1** (3 mmol) and **2** (2.5 mmol) were stirred for 3–6 h at ambient temperature in 5 mL of CH_2Cl_2. After evaporation of the solvent at reduced pressure, the remaining solid was washed with ether (10 mL × 3) to remove excess **1**, dissolved in 10 mL of CH_2Cl_2, and filtered through a Celite pad. **3** was precipitated from the filtrate by the addition of ether. Analytically pure samples were obtained by recrystallization from CH_2Cl_2–Et_2O. **3a**: 65% yield; deep purple-red crystals; mp 127 °C; FDMS, *m/z* 573 [$Fp_3(CH_2CO)$]. Anal. Calcd for $C_{23}H_{17}BF_4O_7Fe_3$: C, 41.87; H, 2.60. Found: C, 41.79; H, 2.45. IR: 2047, 2010 (sh), 2000, 1973, 1957 cm^{-1}. **3b**: 56% yield; deep purple-red crystals; mp 114 °C. Anal. Calcd for $C_{24}H_{19}BF_4O_7Fe_3$: C, 42.79; H, 2.84. Found: C, 42.58; H, 2.63. IR: 2057, 2010, 1975 cm^{-1}. **3c + 3d**: 48% yield from **1a**; 58% yield from **1c**; deep purple-red crystals; mp 137 °C. Anal. Calcd for $C_{24}H_{19}BF_4O_7Fe_3$: C, 42.79; H, 2.84. Found: C, 42.37; H, 2.54. IR: 2054, 2020, 2007, 1978, 1967 (sh) cm^{-1}. **3f**: 74% yield from **1a**; 58% yield from **1d**; deep red crystals; mp 118 °C. Anal. Calcd for $C_{28}H_{27}BF_4O_7Fe_3$: C, 46.09; H, 3.70. Found: C, 46.01; H, 3.68. IR: 2035, 2016, 1985, 1978 cm^{-1}. **3g**: 62% yield; deep red crystals; mp 136 °C; FDMS, *m/z* 713 [$FpFp^*_2(CH_2CO)$]. Anal. Calcd for $C_{37}H_{37}BF_4O_7Fe_3 \cdot CH_2Cl_2$: C, 42.72; H, 4.11. Found: C, 42.52; H, 4.08. IR: 2017, 1989, 1972, 1940 cm^{-1}.

Monitoring Adduct Formation and Metal-Exchange Reaction by ^1H NMR. **1** (0.10 mmol) and **2** (0.10 mmol) were placed in an NMR tube. After the addition of CD_2Cl_2 (0.50 mL) [*t* = 0], the tube was capped with a rubber septum and centrifuged (4000 rpm for 5 min) after sonification (Bransonic 12, 45 kHz/35 W). The supernatant was transferred to another NMR tube by a syringe. The tube was then sealed, and the ^1H NMR spectra were recorded at appropriate time intervals.

Reaction of 3a with Nucleophiles. PPh_3. **3a** (65 mg, 0.1 mmol) and PPh_3 (39 mg, 0.15 mmol) in 0.5 mL of CD_2Cl_2 were sealed in an NMR tube. After 1 h the ^1H NMR spectrum indicated the formation of **1a** and $Fp^+(PPh_3)$ in quantitative yields. IR spectra of ether-soluble and -insoluble parts also supported their structures.

$NaBH_4$. As soon as **3a** (65 mg, 0.1 mmol) and $NaBH_4$ (10 mg, 0.26 mmol) were sealed in THF-d_8 (0.5 mL) in an NMR tube, the mixture turned into yellow. The formation of **1a** was observed by the ^1H NMR spectrum. The mixture gradually changed to

(22) (a) Herrmann, W. A.; Huber, M. *Chem. Ber.* **1978**, *111*, 3124. (b) Macomber, D. W.; Hart, W. P.; Rausch, M. D. *Adv. Organomet. Chem.* **1982**, *21*, 1.
(23) Negishi, E. *Organometallics in Organic Synthesis*; Wiley: New York, 1980; Vol. 1, p 54.
(24) (a) Labadie, S. S.; Stille, J. K. *Tetrahedron* **1984**, *40*, 2329. (b) Kawanisi, M.; Kozima, S.; Kobayasi, K.; Hitomi, T. *Rep. Asahi Glass Found. Ind. Technol.* **1984**, *44*, 109. (c) Koboyasi, K.; Kawanisi, M.; Hitomi, T.; Kozima, S. *Chem. Lett.* **1984**, 497.
(25) Ferguson, G. S.; Wolczanski, P. T. *J. Am. Chem. Soc.* **1986**, *108*, 8293 and references cited therein.
(26) Reger, D. L.; Coleman, C. *J. Organomet. Chem.* **1977**, *131*, 153.
(27) Cathline, D.; Astruc, D. *Organometallics* **1984**, *3*, 1094.
(28) King, R. B. *Organometallic Synthesis*; Academic: New York, 1965; Vol. 1.
(29) Wright, M. E.; Nelson, G. O. *J. Organomet. Chem.* **1984**, *263*, 371.
(30) Samuel, E.; Rausch, M. D. *J. Am. Chem. Soc.* **1973**, *95*, 6263.
(31) Akita, M.; Kakinuma, N.; Moro-oka, Y. *J. Organomet. Chem.* **1988**, *348*, 91.

deep purple (the color of Fp_2). We could not detect any other organic products.

Preparation of Enolate Complexes 6c,d and 8c,d. 1,3-Dioxolanes (acetals) of α-halo ketones were prepared by the published method.[32] NaFp or Na/KFp* (10 mmol) in THF (10 mL) was added to a THF solution (20 mL) of appropriate 1,3-dioxolane (12 mmol) at −78 °C. After the mixture was stirred for 3 h at room temperature, the volatiles were removed under reduced pressure. The product was extracted with ether (100 mL) and filtered through silica gel. The acetal linkage was hydrolyzed by stirring with 1/10 N HCl(aq), and then the organic layer was dried over $MgSO_4$. **6** and **8** were isolated by column chromatography followed by recrystallization from Et_2O. **6c**: 50% yield. **6d**: 48% yield; yellow prisms; mp 90 °C. Anal. Calcd for $C_{16}H_{14}O_4Fe$: C, 58.93; H, 4.33. Found: C, 59.27; H, 4.48. IR: 2004, 1961 cm^{-1}. **8c**: 46% yield; yellow prisms; mp 118 °C. Anal. Calcd for $C_{20}H_{22}O_3Fe$: C, 65.59; H, 6.06. Found: C, 65.62; H, 6.09. IR: 1988, 1937 cm^{-1}. **8d**: 45% yield; yellow prisms; mp 105 °C. Anal. Calcd for $C_{21}H_{24}O_4Fe$: C, 63.65; H, 6.10. Found: C, 63.82; H, 6.08. IR: 1995, 1946 cm^{-1}.

Preparation of 8b. **8b** was prepared according to the published method by using Na/KFp* in place of NaFp. **8b**: 41% yield; yellow crystals; mp 110 °C. Anal. Calcd for $C_{14}H_{18}O_3Fe$: C, 57.95; H, 6.25. Found: C, 58.30; H, 6.41. IR: 1990, 1940 cm^{-1}.

Preparation of Diiron Enolate Complexes 7 and 9. **7** and **9** were prepared in a similar manner to **3**. **7a**: 72% yield; deep red crystals; mp 119 °C; FDMS, m/z 497 [FpFp*(CH_2CO_2Me)] Anal. Calcd for $C_{22}H_{25}BF_4O_6Fe_2$: C, 46.52; H, 4.44. Found: C, 46.68; H, 4.50. IR: 2018, 2001, 1977, 1959 cm^{-1}. **7b**: 63% yield; deep red crystals; mp 126 °C; FDMS, m/z 467 [FpFp*(CH_2CHO)] Anal. Calcd for $C_{21}H_{23}BF_4O_5Fe_2$: C, 45.54; H, 4.18. Found: C, 45.80; H, 4.20. IR: 2032, 1983 cm^{-1}. **7c**: 63% yield; deep red crystals; mp 118 °C; FDMS, m/z 543 [FpFp*(CH_2COPh)] Anal. Calcd for $C_{27}H_{27}BF_4O_5Fe_2$: C, 51.47; H, 4.32. Found: C, 51.58; H, 4.25. IR: 2032 (sh), 2024, 1981, 1973 (sh) cm^{-1}. **7d**: 42% yield; deep red oil. Anal. Calcd for $C_{28}H_{29}BF_4O_6Fe_2$: C, 50.95; H, 4.43. Found: C, 51.46; H, 4.58. **9a**: 52% yield; deep red crystals; mp 88 °C; FDMS, m/z 467 [FpFp*(CH_2CHO)] Anal. Calcd for $C_{22}H_{25}BF_4O_6Fe_2$: C, 46.52, H, 4.44. Found: C, 46.18; H, 4.21. IR: 2060, 2012, 1996, 1948 cm^{-1}. **9b**: 58% yield; deep red crystals; mp 122 °C. Anal. Calcd for $C_{21}H_{23}BF_4O_6Fe_2$: C, 45.54; H, 4.18. Found: C, 45.62; H, 4.23. IR: 2061, 2011, 2000 (sh), 1956 cm^{-1}.

Preparation of 11. To a CH_2Cl_2 solution (10 mL) of Cp_2ZrMe_2 (454 mg, 1.8 mmol) was added to **10** (816 mg, 1.5 mmol)[7c] dissolved in 5 mL of CH_2Cl_2. After gas evolution had ceased, hexane (20 mL) was added. During the removal of the volatiles **11** precipitated as an orange solid, which was collected. Owing to its sensitivity to moisture, an analytically pure sample of **11** could not be obtained. **11**: 58% yield; orange solid; mp 137 °C.

Reaction of 12 with 2a. **12** (998 mg, 2.75 mmol) and **2** (836 mg, 2.50 mmol) were stirred in CH_2Cl_2 (40 mL). After 1 and 72 h a 10-mL portion of the mixture was separated and evaporated to dryness. After being washed with ether, the solid was dissolved in CH_2Cl_2 and treated with PPh_3 (1.5 equiv) for 15 min. Then, the volatiles were removed in vacuo. The product ratio **12**/**6c** was determined by ^1H NMR after extraction with ether.

Acknowledgment. We are grateful to the Asahi Glass Foundation for Industrial Technology and the Ministry of Education, Science and Culture of the Japanese Government for financial support of this research. We thank Mr. Hideki Omori for FDMS measurements.

Registry No. **1a**, 107040-55-1; **1b**, 107040-56-2; **1c**, 111615-23-7; **1d**, 118377-80-3; **2a**, 63313-71-3; **2b**, 116037-29-7; **2c**, 112617-73-9; **3a**, 116017-02-8; **3b**, 118398-15-5; **3c**, 116037-31-1; **3d**, 116017-04-0; **3e**, 118398-17-7; **3f**, 118398-19-9; **3g**, 118398-21-3; **6a**, 12214-69-6; **6b**, 55337-26-3; **6c**, 12319-47-0; **6d**, 118377-81-4; **7a**, 118377-86-9; **7b**, 118377-88-1; **7c**, 118377-90-5; **7d**, 118377-92-7; **8a**, 118378-01-1; **8b**, 118377-84-7; **8c**, 118377-82-5; **8d**, 118377-83-6; **9a**, 118377-94-9; **9b**, 118377-96-1; **9c**, 118377-98-3; **9d**, 118378-00-0; **10**, 111582-14-0; **11**, 116100-36-8; **12**, 12319-80-1; Cp_2ZrMe_2, 12636-72-5.

(32) Visweswariah, S.; Prakash, G.; Bhushan, V.; Chandrasekaran, S. *Synthesis* **1982**, 309.

Photochemical Rearrangements of Stable Silenes

Kim M. Baines, A. G. Brook,* R. R. Ford, P. D. Lickiss, A. K. Saxena, W. J. Chatterton, J. F. Sawyer, and B. A. Behnam

Lash Miller Chemical Laboratories, University of Toronto, Toronto M5S 1A1, Canada

Received June 15, 1988

Photolysis of acylsilanes $(Me_3Si)_2RSiCOR'$ (R = Me, *t*-Bu, Ph, Me_3Si; R' = *t*-Bu, Ad, bicyclooctyl, Mes, CEt_3) gave silenes $Me_3SiRSi{=}C(OSiMe_3)R'$, whose subsequent chemistry was dependent on the steric size of the R and R' groups and on their facile photochemical excitation by UV light. Thus when R = Me or Ph and R' = Ad or R = Me_3Si and R' = bicyclooctyl, head-to-head dimerization occurred giving 1,2-disilacyclobutanes, whereas when R = *t*-Bu and R' = Ad or R = Ph and R' = CEt_3, stable silenes were formed. Some of these silenes, e.g. when R = *t*-Bu or Ph, subsequently underwent complex photochemical isomerizations yielding new silenes (observable by NMR spectroscopy for R = *t*-Bu and R' = Ad or R = Ph and R' = CEt_3). Most of the new isomeric silenes ultimately dimerized to give 1,3-disilacyclobutanes by head-to-tail dimerization as expected from their structures. The crystal structures of four of these dimers (details in the following paper) and one silene–methanol adduct (details herein) were determined by X-ray methods, thus unambiguously establishing the structures of the dimers and of their immediate silene precursors. The data reported have been interpreted on the basis that each acylsilane on photolysis formed only one of the two possible silene geometric isomers, which reacted nonstereospecifically when trapped by added methanol since in each case a diastereomeric mixture of methanol adducts was isolated. A dyotropic-like rearrangement from a twisted silene excited state has been proposed as the simplest mechanism possible to account for the silene-to-silene isomerizations, but this has not been confirmed experimentally.

Introduction

The availability of silenes that are stable at room-temperature has made it possible to study some of the chemistry of these species under "normal" mild conditions, e.g. in solution at room temperature (see recent reviews for an outline of these studies[1,2]). Among the reactions that have been studied recently with our family of stable silenes $(Me_3Si)_2Si{=}C(OSiMe_3)R$ (**2**), derived from photolysis of the related acylsilanes $(Me_3Si)_3SiCOR$ (**1**), are [2 + 2]

(1) Brook, A. G.; Baines, K. M. *Adv. Organomet. Chem.* **1986**, *25*, 1.
(2) Raabe, G.; Michl, J. *Chem. Rev.* **1985**, *85*, 419.

0276-7333/89/2308-0693$01.50/0